Effect of concentrated NaCl on catalytic wet oxidation (CWO) of short chain carboxylic acids

Xiaoxia Ou,[a,*] Helen Daly,[a] Sarayute Chansai,[a] Simon Beaumont,[b] Xiaolei Fan,[a] Christopher Hardacre[a]

[a]*Department of Chemical Engineering and Analytical Science, School of Engineering, The University of Manchester, Oxford Road, Manchester, M13 9PL United Kingdom*

[b] *Department of Chemistry, University of Durham, South Road, Durham, DH1 3LE, United Kingdom*

Abstract

The effect of concentrated NaCl (200 g L^{-1}) on CWO of oxalic acid and acetic acid over $MnCeO_x$ was investigated at 110 °C and 0.5 MPa O_2 to explore the potential of using CWO for shale gas wastewater treatment. The presence of concentrated NaCl hindered oxalic acid conversion, which from ATR-IR spectroscopy was attributed to the salting out effect increasing the oxalic acid surface coverage with formation of strongly adsorbed intermediates, slowing oxalic acid mineralisation. In addition, the weak adsorption of acetic acid on $MnCeO_x$ was proposed to be responsible for the insignificant conversion with or without NaCl present.

Key words:

Catalytic wet oxidation (CWO), $MnCeO_x$, salt effect, *in situ* ATR spectroscopy

1. Introduction

The complex composition of wastewater produced from shale gas extraction is of significant environmental concern, which can impose increased pressure on global water safety. Hence, the removal of differing pollutants (such as organics and salinity) from produced water is necessary for water recovery [1, 2]. Efficient treatment methods are urgently needed to address this challenging problem, and catalytic wet oxidation (CWO) is an emerging option with reports that 97% chemical oxygen demand (COD) in fracturing flowback fluid can be removed by CWO using a Cu-Cr/activated

* Corresponding author e-mail address: xiaoxia.ou@manchester.ac.uk (X. Ou)

carbon catalyst (10 g L^{-1}) at 250 °C under 2.5 MPa oxygen partial pressure [3].

Due to the high salinity in shale gas wastewater (up to 200 g L^{-1} of Cl^-) [2], the effect of concentrated salt on wastewater treatment deserves specific consideration. A number of studies have found a correlation between the salt and CWO efficiency [4-6], with the salting-out effect found to be an important contributing factor as salt can increase the hydrophobicity of reactant molecules in aqueous solutions [7, 8]. In addition, other salt effects on CWO were reported. For example, competitive adsorption between chloride and formic acid on a Pt surface (in a Pt/ceramic membrane) was found in the CWO system with 0.15 g L^{-1} NaCl, causing a lower oxidation rate compared to the pure water system [4]. In a Fenton oxidation process, when the NaCl concentration is higher than 2.5 g L^{-1}, the chloride ions were found to trap OH radicals to produce less reactive radicals ($\cdot HO_2$), which led to the decreased TOC (total organic carbon) conversion [9]. Conversely, the promoting effect of NaCl was reported in catalytic wet peroxide oxidation (CWPO) of phenol, in which phenol conversion was improved by the addition of NaCl over clay-based [5] and Cu-Ni-Al hydrotalcite catalysts [6]. The improvement was due to Cl^- induced hydrogen peroxide decomposition, leading to improved radical formation. However, it is worth noting that in these studies, relatively low salt concentrations, that is, 0.15–10 g L^{-1} NaCl, were used, not being representative for that typical of produced water from shale gas extraction (about 200 g L^{-1} of Cl^-).

Previously we have reported the investigation of the effect of concentrated NaCl (200 g L^{-1}) on CWO of phenol over $MnCeO_x$ [10]; however, research has yet to investigate the effect of concentrated NaCl on CWO of short chain carboxylic acids. Short chain carboxylic acids are identified as the final intermediate products in CWO of most organic pollutants [11] and the oxidation of short chain carboxylic acids is the rate-controlling step in CWO for COD reduction to meet discharge standards [12]. $MnCeO_x$ shows high catalytic activity in CWO of various organic pollutants (e.g. polyethylene glycol and phenol) in systems without salts due to its abundance of lattice oxygen and oxygen vacancies, providing enhanced redox properties [13-15], however, data about the efficacy of $MnCeO_x$ for CWO of oxalic acid and acetic acid has not received the same attention as substrates such as phenol [16-18]. Therefore, in this study, the effect of concentrated NaCl at 200 g L^{-1} on CWO of oxalic acid and acetic acid over $MnCeO_x$ was studied at 110 °C and 0.5 MPa O_2 (the same conditions used in CWO of phenol [10]). Specially, in situ attenuated total reflection infrared spectroscopy (ATR-IR) was performed to

gain insight into the effect of the concentrated salt on CWO of short-chain carboxylic acids, which is beneficial to the development of practical CWO systems for shale gas wastewater treatment.

2. Experimental

Information regarding the preparation and characterisation of the $MnCeO_x$ catalyst (**Fig. S1**) is provided in the Supporting Information (SI).

2.1 CWO

CWO of oxalic acid and acetic acid was carried out in a Parr autoclave reactor (model: 4598) at 110 °C, 0.5 MPa and 600 rpm. The initial concentration of oxalic acid/acetic acid and the $MnCeO_x$ catalyst was at 1 g L^{-1}. NaCl concentration of 200 g L^{-1} was used to simulate shale gas wastewater. Before reaction, the reactor was purged with N_2 and then heated to 110 °C. Once the temperature reached 110 °C, the reactor was purged with O_2 and pressurised to 0.5 MPa of O_2. After the temperature was stable, the stirring was started to initiate the reaction, and the first sample was taken, which was referred to as time zero (t = 0). During the catalytic reaction, samples were withdrawn periodically to follow the extent of CWO (as detailed in SI).

2.2 In situ ATR-IR

$MnCeO_x$ in water slurry was deposited onto ZnSe crystals, and dried at room temperature (RT) overnight to prepare the catalyst layer. A PIKE ATRMaxII accessory with an in-house made ATR flow cell housed in a Bruker Tensor II spectrometer was used to record ATR-IR spectra in situ. A flow of O_2 saturated water or O_2 saturated salt water (NaCl concentration: 200 g L^{-1}) was introduced to flow over the catalyst layer in the ATR flow cell which was heated from RT to 95 °C. At 95 °C, solutions of oxalic acid (1.0 and 2.3 g L^{-1}) or acetic acid (6.0 g L^{-1}) in O_2 saturated water or O_2 saturated salt water were introduced to flow over the catalyst layer, and IR spectra were recorded (8 scans, resolution of 4 cm^{-1}). A spectrum of the catalyst layer before its exposure to any liquids was taken as the background.

3. Results and Discussion

3.1 CWO of oxalic acid

3.1.1 CWO performance

To probe the intrinsic oxidation ability of $MnCeO_x$, control experiments of catalytic degradation of oxalic acid were performed in water (**Figs. 1 and S2**). In the presence of $MnCeO_x$, the oxalic acid conversion at RT was found to be between 42–44% irrespective of the atmosphere (N_2/O_2). This catalytic activity is attributed to the reaction between adsorbed oxalic acid and lattice oxygen of $MnCeO_x$, showing good oxygen mobility and storage capacity of the catalyst [19-21]. This is confirmed as reaction without a catalyst under N_2 gave 2.8% conversion while with reduced $MnCeO_x$ and non-reducible metal oxide, γ–Al_2O_3, only 18.6% and 11.5% conversions of oxalic acid were attained (**Fig 1**). The oxalic acid conversion under N_2 at RT also correlated with the oxalic acid to catalyst ratio (**Fig S3**). The increase in the active sites number enhanced the oxalic acid conversion, which suggested a Mars-van Krevelen mechanism for the oxidation of adsorbed oxalic acid on $MnCeO_x$ under these conditions. Interestingly, increasing the temperature to 110 °C increased the oxalic acid conversion under N_2 to 59.8% and under O_2 to 100%, which suggested an important role of reaction temperature for lattice oxygen mobility and oxygen activation (**Fig 1**).

For comparison, reaction over $MnCeO_x$ under N_2 at RT in salt water was performed and the system without NaCl showed better performance with respect to both oxalic acid and TOC conversions (at 44.2% and 44.0%, respectively, after 2 h) compared to the system with NaCl (38.2% and 36.1%, **Fig. S2**), the reduced conversion under such mild conditions where the catalyst provides the oxygen suggests NaCl is altering the interaction of oxalic acid on the catalyst surface.

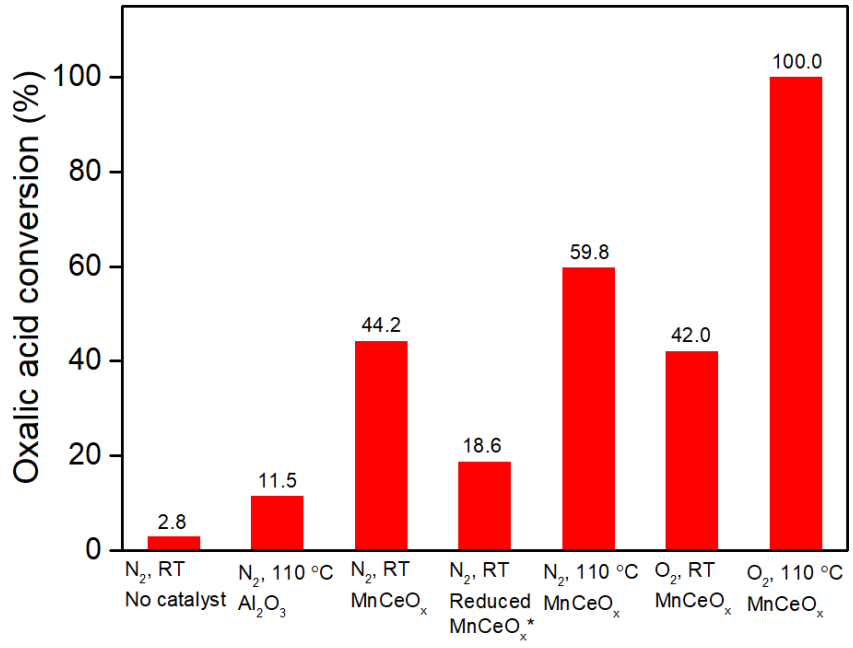

Fig. 1. Oxalic acid conversions at various reaction conditions ($C_{\text{oxalic acid}}$ = 1.0 g L^{-1}, C_{catalyst} = 1.0 g L^{-1}, P = 0.5 MPa). *Reduced $MnCeO_x$: the $MnCeO_x$ catalyst was reduced by H_2 in the Parr autoclave reactor at 250 °C for 4 h before the CWO of oxalic acid.

The activity of $MnCeO_x$ in CWO of oxalic acid was further studied, as shown in **Fig. 2a**. In the system without NaCl, complete oxalic acid conversion was observed in 2 h with a TOC removal of 94.2% (**Fig. S4**). Conversely, in the presence of NaCl, the activity was inhibited, as evidenced by the reduced oxalic acid (71.2%) and TOC conversions (62.0%) after 2 h. By increasing the reaction time to 24 h, the TOC conversion increased to 95.0% in the absence of NaCl while the oxalic acid and TOC conversions increased to 90.1% and 89.5% respectively, in the presence of NaCl (**Fig.2**). Mn leaching was noted in CWO of oxalic acid but was unlikely the cause of the lower activity in the presence of NaCl (see SI). Insignificant carbonaceous deposits (~0.2 mg) were found in the used $MnCeO_x$ catalysts after reactions for 24 h, which along with the high oxalic acid and TOC conversions achieved, indicated that $MnCeO_x$ catalysts were active for oxalic acid mineralisation in the presence of NaCl although a longer reaction time was needed to achieve mineralisation (see carbon balance in SI).

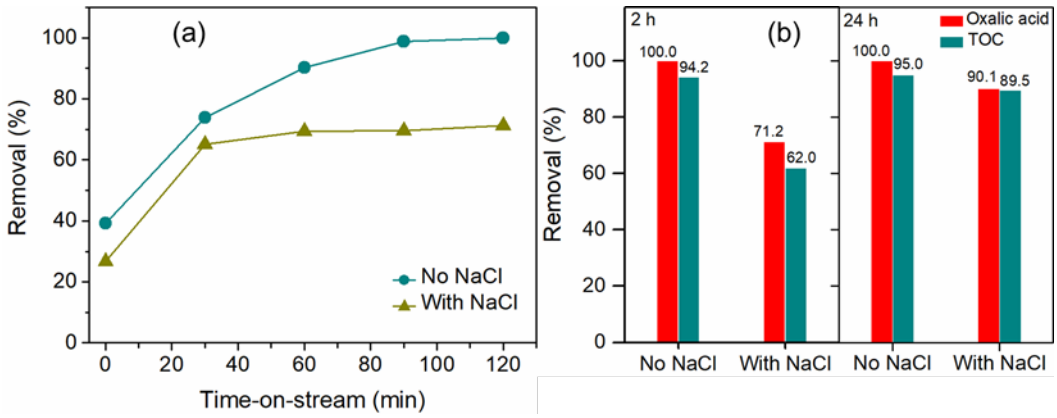

Fig. 2. (a) Conversion of oxalic acid as a function of time-on-stream (2 h reaction); (b) Conversions of oxalic acid and TOC after 2 h and 24 h reaction (reaction conditions: $C_{\text{oxalic acid}}$ = 1.0 g L^{-1}, C_{catalyst} = 1.0 g L^{-1}, T = 110 °C, P_{O2} = 0.5 MPa).

3.1.2 In situ ATR-IR of adsorption/CWO of oxalic acid on $MnCeO_x$

In situ ATR spectra of 1 g L^{-1} oxalic acid in water/O_2 and salt water/O_2 over $MnCeO_x$ at 95 °C are shown in **Fig. 3**. Adsorption of oxalic acid on $MnCeO_x$ in water resulted in spectra with bands at 1709 and 1691 cm^{-1} assigned to C=O stretching vibrations and bands at 1424 and 1253 cm^{-1} assigned to stretching vibrations of C–O/C–C/O–C=O bonds and bending mode of O–C=O of adsorbed oxalate [22-25]. The two C=O bands are assigned to individual monoprotonated species (HO_x^-) adsorbed in a monodentate or bidentate adsorption mode (**Fig. S5**) [22-25]. The adsorption of oxalic acid in water/O_2 at 95 °C (**Fig 3a**) also exhibited weak bands at 1599 and 1309 cm^{-1} (along with bands at ~1660 and 1460 cm^{-1}) due to chemisorbed oxalic acid species (see SI). The adsorption of oxalic acid on $MnCeO_x$ at 95 °C in salt water exhibited comparable spectra during initial exposure of the catalyst to the solution (**Fig 3b**), however, longer exposure time brought a significant increase in intensity of bands at 1600 (peak maximum shifting to lower wavenumber with increasing coverage) and 1310 cm^{-1} along with increased intensity of bands at 1456, 1367 and 1299 cm^{-1} (**Fig 3c**). As these bands increased, the band at 1715 cm^{-1} decreased in intensity indicating the loss of a weakly adsorbed monoprotonated oxalic acid species.

After exposure of $MnCeO_x$ to the oxalic acid salt water/O_2 (or water/O_2) solution, the flow was switched to salt water/O_2 (or water/O_2) to probe the strength of adsorption of oxalic acid on the catalyst. **Fig. S6** shows that salt water/O_2 flow did not have a significant effect on the intensity of bands due to adsorbed oxalic acid species with only a small initial decrease in intensity of the C=O bands at 1715 and 1691

cm^{-1} observed. The adsorbed oxalic acid species which formed at increased exposure time (higher surface coverage) were strongly bound to the catalyst. Contrastingly, a faster decrease in intensity of all bands was observed in water/O_2.

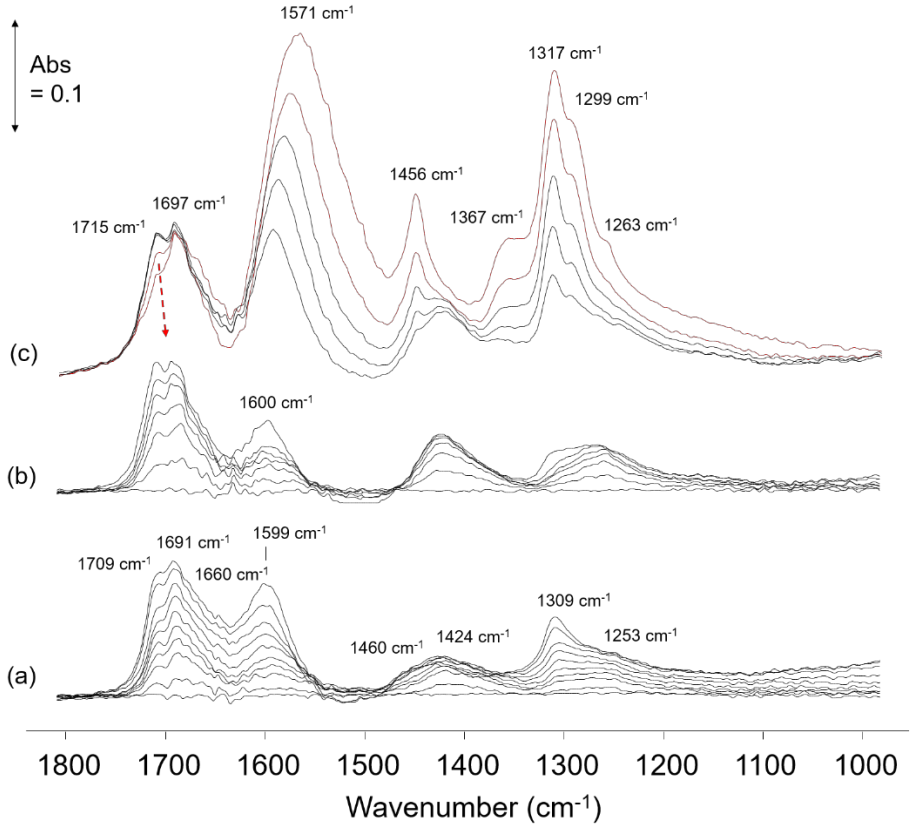

Fig 3. ATR spectra of 1 g L^{-1} oxalic acid adsorption on $MnCeO_x$ at 95 °C in (a) water/O_2 (10 minutes exposure to the oxalic acid solution) and (b) salt water/O_2, 0–2.5 minutes exposure to the oxalic acid solution and (c) salt water/O_2, 2.5–12 minutes exposure to the oxalic acid solution. Bands due to water have been subtracted from all spectra.

As the strongly bound species formed in salt water at longer exposure time, a higher concentration of oxalic acid (2.3 g L^{-1}) in water/O_2 solution was studied, as shown in **Fig 4**. Interestingly, adsorption at RT did not result in the formation of intense bands at 1600, 1479, 1360 and 1310 cm^{-1} with little change in bands (1714, 1691 and 1253 cm^{-1}) intensity observed after 15 mins exposure, indicating surface saturation was reached at RT with this higher concentration of oxalic acid. These species were also weakly bound, decreasing in intensity under a water/O_2 flow at RT (**Fig S7**).

However, introduction of 2.3 g L^{-1} oxalic acid solution at 95 °C did not reach surface saturation within

15 minutes with promoted formation of bands at 1668, 1596, 1471, 1360 and 1311 cm^{-1} (**Fig 4b**). The bands observed after 15 mins exposure to 2.3 g L^{-1} oxalic acid/water/O_2 were at similar positions to those formed from adsorption of 1 g L^{-1} oxalic acid in salt water (both at 95 °C). The presence of salt increased the adsorption of oxalic acid on the catalyst indicated a salting out effect of NaCl, which increased the coverage of oxalic acid on the catalyst. As the coverage increased (in salt water or higher oxalic acid concentrations in water), bands at 1668, 1596, 1471, 1360 and 1311 cm^{-1} were observed. These species could be due to the formation of intermediates on the catalyst such as formate (**Fig S8**), carboxylate (νCOO_{asym} and νCOO_{sym} bands) or carbonate species. These strongly adsorbed intermediate species on the catalyst in salt water would be slower to oxidise to CO_2, which correlates with the slower mineralisation of oxalic acid observed in the activity testing.

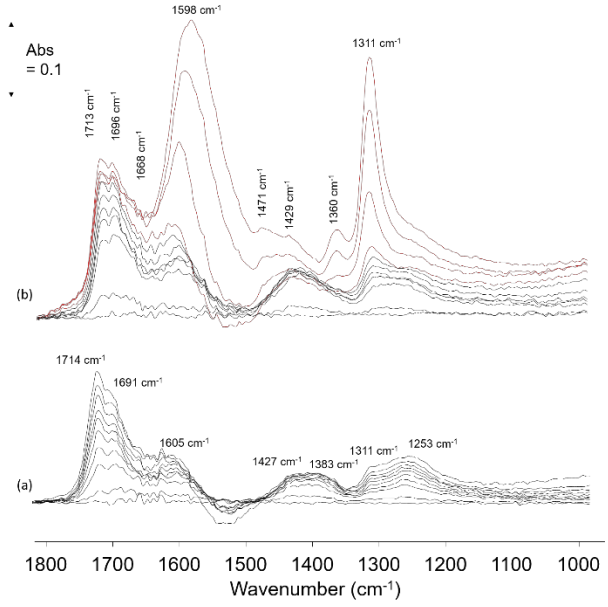

Fig 4: ATR spectra of $MnCeO_x$ after 15 minutes exposure to a 2.3 g L^{-1} oxalic acid/water/O_2 at (a) RT and (b) 95 °C. Bands due to water have been subtracted from all spectra.

3.2 CWO of acetic acid

Acetic acid is considered as the most refractory pollutant among carboxylic acids (acetic, oxalic and formic acids) [18]. Though $MnCeO_x$ has been reported to show activity in CWO of acetic acid at 150 °C and 0.9 MPa O_2 pressure [18], insignificant acetic acid conversion was observed in the conditions used

for CWO of oxalic acid herein ($C_{carboxylic\ acid}$ = 1.0 g L^{-1}, $C_{catalyst}$ = 1.0 g L^{-1}, T = 110 °C, P_{O2} = 0.5 MPa). In detail, acetic acid conversion was 3.7% and 3.9% (error ~2.0%) after 24 h when $MnCeO_x$ was present with and without NaCl, respectively, while TOC conversion was 3.2% and 2.2% (error ~1.0%), respectively, indicating that mineralisation of acetic acid was not observed in either system as shown by the carbon balance in the SI.

ATR spectra of acetic acid adsorbed on $MnCeO_x$ in water and salt water at 95 °C are shown in **Fig. 5a**. Bands due to molecularly adsorbed acetic acid were observed at 1728 cm^{-1} due to ν(C=O) and 1415 and 1272 cm^{-1} which are in comparable positions to H-bonded acetic acid on TiO_2 [26]. Bands due to acetate species were observed at 1557 and 1528 cm^{-1} due to ν_{asym}(C=O) and at 1444 and 1418 cm^{-1} due to the ν_{sym}(C=O) vibration of different acetate species. These could be due to species adsorbed on different sites of $MnCeO_x$ with the difference in wavenumber associated with the asymmetric and symmetric vibrations of the carboxylate bands, indicating bridging bidentate (or chelating) acetate species on $MnCeO_x$ under these conditions [27].

Upon switching from the acetic acid/water/O_2 feed to water/O_2, bands in the spectra decreased at different rates (**Fig. 5b**) with an initial loss of features due to dissolved/molecularly adsorbed acetic acid before disappearance of bands associated with acetate species. As the acetate band intensity decreased under the water/O_2 flow, bands due to the molecularly adsorbed acetic acid were then observed to increase. This is in line with studies of Liao *et al.* on photodecomposition of acetic acid where the presence of water was reported to convert acetate species back to acetic acid [26]. The weak adsorption seen here is in good agreement with weak adsorption of acetic acid reported for other oxides such as TiO_2 [28]. The mode of adsorption and substrate surface coverage have been shown to influence the rate of mineralisation of oxalic acid (and phenol) and concentrated NaCl altered the surface coverage of the substrates (salting out with an increase for oxalic acid and site blocking with reduction of carbonaceous deposits for phenol [10]). The effect of NaCl on acetic acid oxidation over $MnCeO_x$ was trivial under the current CWO conditions with the weak adsorption of acetic acid in water on $MnCeO_x$ proposed to be the cause of the low conversion/mineralisation with concentrated NaCl having little effect on the substrate adsorption/surface coverage.

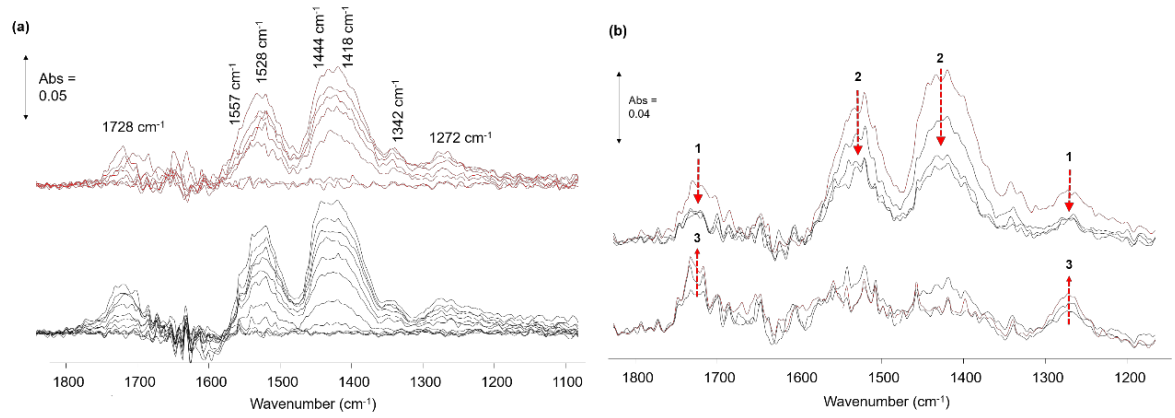

Fig. 5. ATR spectra over $MnCeO_x$ at 95 °C as a function of exposure time (a) under a flow of acetic acid in O_2 saturated water (black spectra) and salt water (red water) and (b) on switching from acetic acid in water/O_2 to a flow of water/O_2 to monitor the strength of acetate adsorption on $MnCeO_x$. Bands due to water have been subtracted.

Conclusions

Short-chain carboxylic acids can be the main target pollutants in CWO for wastewater treatment. To explore the potential of CWO for shale gas wastewater treatment, CWO of oxalic acid and acetic acid in the presence of concentrated NaCl (200 g L^{-1}) was investigated. Regarding oxalic acid, 100% oxalic acid and 94.2% TOC removals were observed in water over $MnCeO_x$ after 2 h, whilst the presence of concentrated NaCl reduced the rate of oxalic acid oxidation, resulting in the reduced oxalic acid and TOC removal of 71.2% and 62.0%, respectively, which increased at longer reaction times, reaching 90.1% and 89.5% after 24 h. The reduced conversion/mineralisation of oxalic acid in salt water could be due to the formation of strongly bound intermediates at higher oxalic acid coverage which result from salting out of oxalic acid on the catalyst in salt water. For acetic acid, insignificant removals (3.9% and 3.7% in the absence and presence of NaCl) over $MnCeO_x$ were observed, which was attributed to the weak adsorption of acetic acid on the catalyst.

Acknowledgements

UK Catalysis Hub is kindly thanked for resources and support provided via our membership of the UK Catalysis Hub Consortium and funded by EPSRC grant: EP/R026939/1, EP/R026815/1, EP/R026645/1, EP/R027129/1.

References

[1] J.M. Estrada, R. Bhamidimarri, A review of the issues and treatment options for wastewater from shale gas extraction by hydraulic fracturing, Fuel, 182 (2016) 292-303.

[2] N.R. Warner, C.A. Christie, R.B. Jackson, A. Vengosh, Impacts of shale gas wastewater disposal on water quality in western Pennsylvania, Environ Sci Technol, 47 (2013) 11849-11857.

[3] Y. Liu, D. Wu, M. Chen, L. Ma, H. Wang, S. Wang, Wet air oxidation of fracturing flowback fluids over promoted bimetallic Cu-Cr catalyst, Catalysis Communications, 90 (2017) 60-64.

[4] I. Kumakiri, R. Bredesen, Meso-porous catalytic membrane contactors applied for organic oxidation in salty water, Advanced Science Letters, 19 (2013) 601-604.

[5] S. Zhou, C. Zhang, R. Xu, C. Gu, Z. Song, M. Xu, Chloride ions promoted the catalytic wet peroxide oxidation of phenol over clay-based catalysts, Water Sci Technol, 73 (2016) 1025-1032.

[6] S. Zhou, Z. Qian, T. Sun, J. Xu, C. Xia, Catalytic wet peroxide oxidation of phenol over Cu–Ni–Al hydrotalcite, Applied Clay Science, 53 (2011) 627-633.

[7] N.N. Mahamuni, A.B. Pandit, Effect of additives on ultrasonic degradation of phenol, Ultrason Sonochem, 13 (2006) 165-174.

[8] A. Kumar, Salt effects on Diels-Alder reaction kinetics, Chem Rev, 101 (2001) 1-19.

[9] R. Maciel, G.L. Sant'Anna, Jr., M. Dezotti, Phenol removal from high salinity effluents using Fenton's reagent and photo-Fenton reactions, Chemosphere, 57 (2004) 711-719.

[10] H.D. X. Ou, X. Fan, S. Beaumont, S. Chansai, A. Garforth, S. Xu, C. Hardacre, High ionic strength wastewater treatment by catalytic wet oxidation (CWO) over $MnCeO_x$ catalyst, Unpublished results.

[11] K.H. Kim, S.K. Ihm, Heterogeneous catalytic wet air oxidation of refractory organic pollutants in industrial wastewaters: a review, J Hazard Mater, 186 (2011) 16-34.

[12] R.V. Shende, V.V. Mahajani, Kinetics of wet air oxidation of glyoxalic acid and oxalic acid, Ind. Eng. Chem. Res., 33 (1994) 3125-3130.

[13] S. Imamura, M. Nakamura, N. Kawabata, J. Yoshida, S. Ishida, Wet oxidation of poly (ethylene glycol) catalyzed by manganese-cerium composite oxide, Industrial & engineering chemistry product research and development, 25 (1986) 34-37.

[14] S. Hamoudi, F. Larachi, G. Cerrella, M. Cassanello, Wet oxidation of phenol catalyzed by unpromoted and platinum-promoted manganese/cerium oxide, Ind. Eng. Chem. Res., 37 (1998) 3561-3566.

[15] H. Chen, A. Sayari, A. Adnot, F.ç. Larachi, Composition–activity effects of Mn–Ce–O composites on phenol catalytic wet oxidation, Appl. Catal. B-Environ., 32 (2001) 195-204.

[16] S. IMAMURA, H. NISHIMURA, S. ISHIDA, Preparation of Mn/Ce composite oxide catalysts for the wet oxidation of acetic acid and their catalytic activities, Journal of The Japan Petroleum Institute, 30 (1987) 199-202.

[17] Z. Jeirani, J. Soltan, Ozonation of oxalic acid with an effective catalyst based on mesoporous MCM-41 supported manganese and cerium oxides, J. Water Proc.engineering, 12 (2016) 127-134.

[18] F. Arena, C. Italiano, G.D. Ferrante, G. Trunfio, L. Spadaro, A mechanistic assessment of the wet air oxidation activity of MnCeOx catalyst toward toxic and refractory organic pollutants, Appl. Catal. B-Environ., 144 (2014) 292-299.

[19] B. Hu, C.-h. Chen, S.J. Frueh, L. Jin, R. Joesten, S.L. Suib, Removal of Aqueous Phenol by Adsorption and Oxidation with Doped Hydrophobic Cryptomelane-Type Manganese Oxide (K−OMS-2) Nanofibers, J. Phys. Chem. C, 114 (2010) 9835-9844.

[20] F. Arena, J. Negro, A. Parmaliana, L. Spadaro, G. Trunfio, Improved MnCeOxSystems for the Catalytic Wet Oxidation (CWO) of Phenol in Wastewater Streams, Ind. Eng. Chem. Res., 46 (2007) 6724-6731.
[21] F. Arena, Multipurpose composite MnCeO x catalysts for environmental applications, Catal. Sci. Technol., 4 (2014) 1890-1898.
[22] S.J. Hug, B. Sulzberger, In situ Fourier transform infrared spectroscopic evidence for the formation of several different surface complexes of oxalate on TiO2 in the aqueous phase, Langmuir, 10 (1994) 3587-3597.
[23] A.G. Young, A.J. McQuillan, Adsorption/desorption kinetics from ATR-IR spectroscopy. Aqueous oxalic acid on anatase TiO2, Langmuir, 25 (2009) 3538-3548.
[24] C.B. Mendive, D.W. Bahnemann, M.A. Blesa, Microscopic characterization of the photocatalytic oxidation of oxalic acid adsorbed onto TiO2 by FTIR-ATR, Catal. Today, 101 (2005) 237-244.
[25] C.B. Mendive, T. Bredow, A. Feldhoff, M.A. Blesa, D. Bahnemann, Adsorption of oxalate on anatase (100) and rutile (110) surfaces in aqueous systems: experimental results vs. theoretical predictions, Physical Chemistry Chemical Physics, 11 (2009) 1794-1808.
[26] L.-F. Liao, C.-F. Lien, J.-L. Lin, FTIR study of adsorption and photoreactions of acetic acid on TiO 2, Physical Chemistry Chemical Physics, 3 (2001) 3831-3837.
[27] F.P. Rotzinger, J.M. Kesselman-Truttmann, S.J. Hug, V. Shklover, M. Grätzel, Structure and vibrational spectrum of formate and acetate adsorbed from aqueous solution onto the TiO2 rutile (110) surface, The Journal of Physical Chemistry B, 108 (2004) 5004-5017.
[28] I. Dolamic, T. Bürgi, Photocatalysis of dicarboxylic acids over TiO2: An in situ ATR-IR study, J. Catal, 248 (2007) 268-276.